AMERICAN SOCIETY FOR MICROBIOLOGY | Antimicrobial Agents and Chemotherapy®

MECHANISMS OF RESISTANCE

Daptomycin Resistance in *Enterococcus faecium* Can Be Delayed by Disruption of the LiaFSR Stress Response Pathway

Amy G. Prater,[a] Heer H. Mehta,[a] Kathryn Beabout,[a] Adeline Supandy,[a] William R. Miller,[b,c] Truc T. Tran,[b,c] Cesar A. Arias,[b,c,d,e] Yousif Shamoo[a]

[a]Department of BioSciences, Rice University, Houston, Texas, USA
[b]Center for Antimicrobial Resistance and Microbial Genomics and Division of Infectious Diseases, UTHealth McGovern Medical School, Houston, Texas, USA
[c]Center for Infectious Diseases, UTHealth School of Public Health, Houston, Texas, USA
[d]Molecular Genetics and Antimicrobial Resistance Unit, International Center for Microbial Genomics, Universidad El Bosque, Bogotá, Colombia
[e]Department of Microbiology and Molecular Genetics, UTHealth McGovern Medical School, Houston, Texas, USA

ABSTRACT LiaFSR signaling plays a major role in mediating daptomycin (DAP) resistance in enterococci, and the lack of a functional LiaFSR pathway leads to DAP hypersusceptibility. Using *in vitro* experimental evolution, we evaluated how *Enterococcus faecium* with a *liaR* response regulator gene deletion evolved DAP resistance. We found that knocking out LiaFSR signaling significantly delayed the onset of resistance, but resistance could emerge eventually through various alternate mechanisms that were influenced by the environment.

KEYWORDS *Enterococcus*, antibiotic resistance, daptomycin, drug resistance evolution

Daptomycin (DAP) is a cyclic lipopeptide antibiotic used to treat multidrug-resistant Gram-positive infections (1–3). Changes in the LiaFSR signaling pathway contribute to resistance in both *Enterococcus faecalis* and *Enterococcus faecium* (4–10). The occurrence of LiaFSR adaptive mutations across enterococci suggests that inhibition of LiaFSR signaling in conjunction with DAP may extend clinical DAP efficacy by inducing hypersusceptibility to the antibiotic and delaying the evolution of resistance, (9, 11, 12).

Previously, we determined that DAP-tolerant *E. faecium* isolates containing LiaFSR-activating alleles can achieve high levels of DAP resistance via a range of evolutionary trajectories (13). Because additional resistance mechanisms are accessible to *E. faecium*, it was important to establish whether *E. faecium* lacking a functional LiaFSR system would be able to rapidly adapt to DAP and thereby undermine the efficacy of any potential LiaFSR inhibitor. To address this concern, two clinical *E. faecium* isolates, HOU503 and HOU515 (7), with deletions of the gene encoding the LiaR response regulators (503FΔ*liaR* and 515FΔ*liaR*, respectively) (6) were evolved to DAP resistance using flask-transfer and bioreactor-mediated experimental evolution (13). Initial DAP MICs in brain heart infusion (BHI) with supplemented calcium (50 mg/liter) were 0.25 and 0.5 mg/liter, respectively. HOU503 and the 503FΔ*liaR* derivative are vancomycin (VAN) resistant, with a VAN MIC of >256 mg/liter, whereas HOU515 and the derivative 515FΔ*liaR* are VAN susceptible.

Five independent populations were evolved via flask transfer, favoring planktonic populations as cells that adhere to surfaces are less likely to be transferred each day. Cells were grown in BHI containing 50 mg/liter calcium, and 100-fold dilutions were transferred daily to increasing DAP concentrations until populations were growing at ≥8 mg/liter DAP (Fig. 1). The 503FΔ*liaR* flask populations reached the MIC threshold within 18 days and the 515FΔ*liaR* flask population in 20 days, compared to the 6 days required for HOU503 (13) and HOU515 containing intact LiaFSR pathways.

Citation Prater AG, Mehta HH, Beabout K, Supandy A, Miller WR, Tran TT, Arias CA, Shamoo Y. 2021. Daptomycin resistance in *Enterococcus faecium* can be delayed by disruption of the LiaFSR stress response pathway. Antimicrob Agents Chemother 65: e01317-20. https://doi.org/10.1128/AAC.01317-20.

Address correspondence to Yousif Shamoo, shamoo@rice.edu.

Received 23 June 2020
Returned for modification 8 August 2020
Accepted 8 January 2021
Accepted manuscript posted online 19 January 2021
Published 18 March 2021

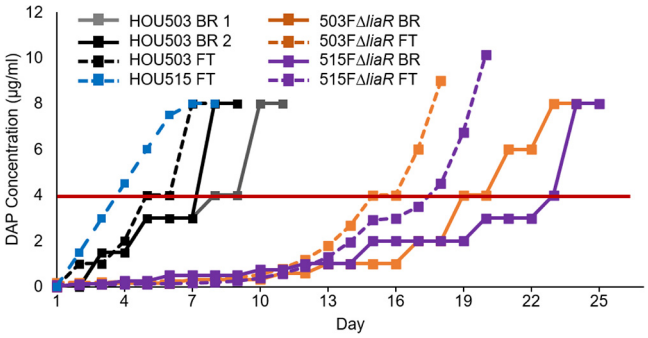

FIG 1 Deleting *liaR* delayed the emergence of DAP resistance. 503FΔ*liaR* and 515FΔ*liaR* were adapted to DAP resistance via flask transfer (FT) (five populations each) or bioreactor (BR) (one population each). Horizontal red line indicates clinical DAP susceptibility cutoff. Each replicate FT population was transferred to identical DAP concentrations. HOU503 data are replotted from Prater et al. (13).

503FΔ*liaR* and 515FΔ*liaR* were also evolved to DAP resistance in singlicate using a bioreactor, which selects for the formation of complex-structured communities that are typically found in biofilms (5, 13, 14). Bioreactor experiments maintain highly polymorphic populations; however, that polymorphism is also highly replicable when the selection is moderate and the population sufficiently large. Previously, replicate bioreactor populations evolved similar mutations, although the frequency at which those mutations occurred varied (15–18). In brief, 200-ml cultures were maintained at mid-log phase in a Sartorius Stedim Biostat B Plus 1-liter vessel. Exhaust CO_2 was measured by a Magellen Tandem Pro gas analyzer to act as a proxy for culture growth rate, where rising CO_2 levels would trigger an influx of fresh medium to maintain a constant turbidity. Every 2 days, a sample of the adapting population was subjected externally to MIC testing in tubes to identify the highest DAP concentration tolerated by the cells. Using these external results, the bioreactor DAP concentration was adjusted. Following this protocol, the 503FΔ*liaR* and 515FΔ*liaR* populations reached ≥8 mg/liter DAP within 23 and 25 days, respectively, compared to the 8 to 10 days required for HOU503 (Fig. 1). Thus, when LiaFSR signaling was disrupted, the time to evolve DAP resistance was more than doubled, regardless of environment.

To identify genetic changes associated with alternative resistance pathways in the absence of LiaFSR signaling, whole-genome sequencing was performed on two random isolates from each of the final flask-transfer populations, the daily bioreactor metapopulations, and phenotypically diverse bioreactor-derived endpoint isolates (13). Flask-transfer isolates were selected randomly because flask populations tend to be less polymorphic than bioreactor populations or those from experiments that form long-term structured communities and biofilms (Tables 1 and 2) (13, 19). Bioreactor-derived isolates were selected nonrandomly to sample a range of MICs, and thus, the frequency of bioreactor endpoint genotypes did not reflect the population frequency (Fig. 2 and Tables 3 and 4). Samples were sequenced by Genewiz with 2 × 150-bp reads on HiSeq. Endpoint isolates were sequenced with a minimum coverage of 100-fold, whereas daily populations were sequenced with at least 300-fold coverage. Illumina sequences were compared with the appropriate closed ancestor genomes (503F_del_LiaR or 515FdelLiaR under BioProject no. PRJNA544687 and PRJNA551139, respectively), using the Breseq genomic pipeline (20).

In a flask environment, two 503FΔ*liaR* and all five 515FΔ*liaR* flask populations contained mutations in *yvcRS* (Tables 1 and 2), the multicomponent system that senses bacitracin and was previously shown to provide DAP resistance in flask-transfer isolates of *E. faecium* HOU503 (13). In HOU503, *yvcRS* mutations were correlated with an increase in *dltABCD* transcripts, an increase in cell surface charge, and a reduction in DAP binding, consistent with the repulsion-based resistance mechanism (13). Here, we

TABLE 1 503FΔ*liaR* flask-transfer endpoint isolate genotypes

Isolate	DAP MIC	Population	VAN Plasmid	*cls*	*yvcS*	*pyre*	*entfae_548*	*nrmA*	*entfae_1207*	*rpoC*	*entfae_357*	*entfae_370*	*entfae_933*	*entfae_1482*	*entfae_2177*	*entfae_2936*
503FΔliaR FT 1-1	32	1	Δ	A20D	A647P											
503FΔliaR FT 1-2	16	1	Δ	A20D	A647P								N73N			
503FΔliaR FT 2-1	8	2	Δ	R218Q		+309	T227R									
503FΔliaR FT 2-2	8	2	Δ	R218Q		+309	T227R				D108Y					
503FΔliaR FT 3-1	>64	3	Δ	A20D										A39S	L303S	T299M
503FΔliaR FT 4-1	32	4	Δ					H105P	Q387K							
503FΔliaR FT 4-2	32	4	Δ					H105P	Q387K							
503FΔliaR FT 5-1	4	5		R211L	W503S					T777K						
503FΔliaR FT 5-2	32	5		R211L	W503S					T777K		L60L				
Total Strains with Changes			7	7	4	2	2	2	2	2	1	1	1	1	1	1

again found that mutations in *yvcRS* occurred, even in the absence of an intact LiaFSR system.

To determine whether cells lacking *liaR* and containing *yvcRS* variants resulted in a similar resistance mechanism, *dltA* transcripts were measured and cell surface qualities quantified. *dltA* transcripts were compared with the housekeeping gene glucose-1-dehydrogenase 4 (*gdhIV*) and were quantified using the $2^{-\Delta\Delta Ct}$ method. Experiments were performed in biological and technical triplicate with the *gdhIV* forward primer (AAGCAGTCTCTGTACAAGCAG) and reverse primer (AGGCTAAGTTCATGGGTTGG) (13). To determine DAP binding patterns, cells were grown to optical density at 600 nm (OD_{600}) 0.5 and then incubated with 32 μg/ml boron-dipyrromethene (BDP):DAP at 37°C with shaking in the dark for 20 min followed by a HEPES wash (7, 10, 13, 21–24). To determine cell surface charge, cells were grown to OD_{600} 0.5 and washed

TABLE 2 515FΔ*liaR* flask-transfer endpoint isolate genotypes

Isolate	DAP MIC	Population	*iacI*	*yvcR*	*yvcS*	*entf515F_1123*	*entf515F_316*	*gap*	*ptsI*	*cls*	*purL*	*entf515F_532*	*entf515F_893*	*entf515F_985*	*entf515F_1120-1125*	*entf515F_1182*	*ccpA*	*entf515F_1885*	*entf515F_2281*	*entf515F_517*	*entf515F_572*	*orf_2425*	*pgsA*	*ptbA*	*entf515F_3084*	*repA* (Plasmid 169)	*entf515F_3134*
515FΔliaR FT 1-2	>64	1		A155D				D314N														+94		-25			
515FΔliaR FT 2-1	64	2	I26V		G579S	Δ		Y180C		R211Q			-43	S96R	Δ4.5 Kb												
515FΔliaR FT 2-2	64	2	I26V		G579S	Δ		Y180C		R211Q			-43	S96R	Δ4.5 Kb										G50G	+500	
515FΔliaR FT 3-1	16	3	I26V	D143N		Y58*			+18								T6-7			K273*							
515FΔliaR FT 3-2	16	3	I26V	D143N		Y58*			+18								T6-7										
515FΔliaR FT 4-1	16	4	I26V		S171L		D57N																-62				
515FΔliaRFT 5-1	32	5	I26V	S209R		T86I	H61Y				I626N	G127A				G489V		A420E	+222								
515FΔliaR FT1 5-2	16	5	I26V	S209R		T86I	H61Y				I626N	G127A				G489V		A420E	+222								+332
Total Strains with Changes			8	5	3	6	3	3	2	2	2	2	2	2	2	2	2	2	2	1	1	1	1	1	1	1	1

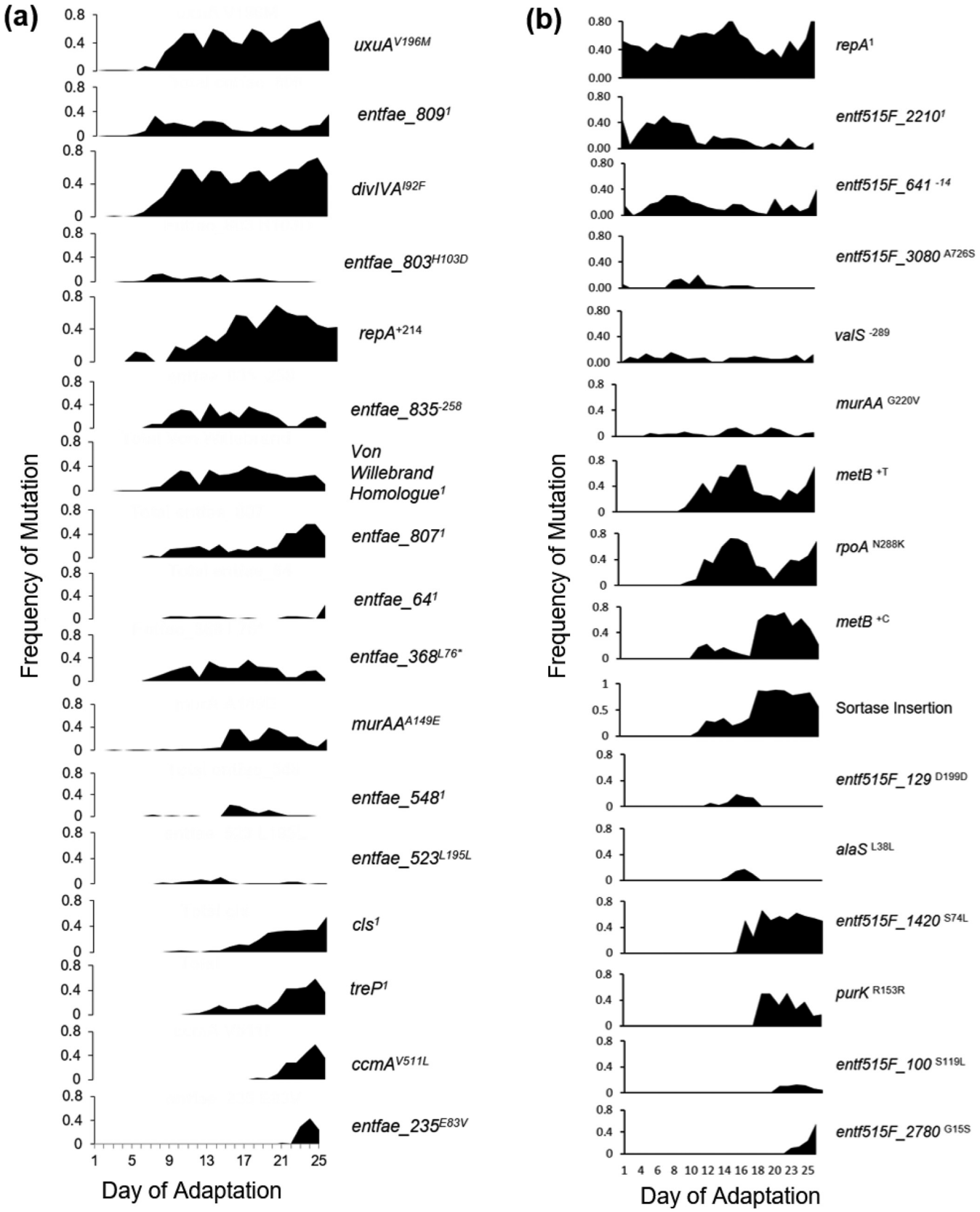

FIG 2 LiaR-independent bioreactor mutation frequencies over time. Mutations that reached a minimum of 10% frequency on 2 consecutive days are included. [1]Multiple mutations were present within that gene, the summation of which is represented here. * indicates mutation resulted in a stop codon. (a) 503FΔ*liaR*. (b) 515FΔ*liaR*. Importantly, mutations unrelated to DAP resistance can accumulate within a population by "hitchhiking" with a bona fide adaptive mutation, such as *uxuA*^{V196M} with *divIVA*^{I92F}, as seen in panel a.

TABLE 3 503FΔ*liaR* bioreactor-derived endpoint isolate genotypes

Isolate	DAP MIC	*cls*	*murAA*	*entfae_809*	*entfae_64*	*entfae_126*	*repA* (Plasmid 1)	*divIVA*	von Willebrand factor homologue type A	*entfae_810*	*entfae_479*	*mfd*	MULE transposase *entfae_497*	*FtsE*	*entfae_1042*	*spxB*	*entfae_2516*	*entfae_2618*
P93	8					V30*												
P62	8	R211L		A70E														E375E
P69	8	R211L		A70E			+214											
P40	8	A20D	A149E	A70E	Y83*													
P59	8	A20D	A149E	A70E	Y83*													
P8	8	A20D	A149E	A70E	Y83*													
P60	8	N13I	A149E			V30*	+214											
P57	8	N13I				V30*	+214		S341R	V52E	R472*	R491*						
P83	4	R211L		A70E														
P33	4	A20D	A149E	A70E	Y83*													
P65	4	A20D	A149E	A70E	Y83*													
P25	4	R211L				V30*		I92F								L394L		
P30	4	N13I	A149E			V30*	+214								A155S		V165V	
P50	4	H215R	A149E	A70E	Y83*								-370	R72C				
P55	4	N13I				V30*	+214		S341R	V52E	R472*	R491						
P70	2	R211L				V30*		I92F		T67M								
P56	2	R267H	A149E			V30*	+214											
P79	2	A20D	A149E	A70E	Y83*													
P49	2	A20D	A149E	A70E	Y83*													
Total Strains with Changes		18	11	11	8	8	6	2	2	3	2	2	1	1	1	1	1	1

three times in HEPES (20 mM, pH 7.0), normalized to OD_{600} 0.1, and incubated with 10 μg/ml poly-L-lysine conjugated to fluorescein isothiocyanate (PLL:FITC) at room temperature for 10 min with shaking followed by a HEPES wash (13, 25). To determine anionic phospholipid distributions, cells were grown to 0.2 and then incu-

TABLE 4 515FΔ*liaR* bioreactor-derived endpoint isolate genotypes

Isolate	DAP MIC	*metB*	*rpoA*	Sortase Insertion (Plasmid 169)	*repA* (Plasmid 169)	*yvcR*	*purK*	*gdpD*	*entf515F_1865*	*entf515F__191*	*fabI*	*entf515F__836*	*rpmG*	*entf515F__1014*	*entf515F__1167*	*entf515F__1188*	*liaY*	*entf515F__1209*	*murAA*	*entf515F__1307*	*entf515F__691*	*dcm*	*entf515F__2481*	Additional Mutations
P29	16	+C		N10*				H29R	A327E															
P36	16	+C		N10*				H29R	A327E															
P69	16	+C		N10*				H29R	A327E															
P31	8	+T	N288K		+501	G15S						G39R	-14	N156S	L87L	E514K	Y74N	V233F	G220V	Y177C		C24Y		
P53	8	+T	N288K		+501	G15S						G39R	-14	N156S	L87L	E514K	Y74N	V233F	G220V	Y177C				
P59	8	+T	N288K		+501	G15S				V336V													+118	
P40	8	+C		N10*			R153R				-108													
P51	4	+T	N288K		+718	G15S				V336V														
P13	4	+T	N288K		+496																			
P62	4	+C		N10*			R153R				-108													
P24	1	+C		L8*			R153R														Δ155 bp			
P86	2											G39R	-14	N156S	L87L	E514K	Y74N	V233F	G220V	Y177C				33
Total Strains with Changes		11	5	6	5	4	3	3	3	2	2	3	3	3	3	3	3	3	3	3	1	1	1	N/A

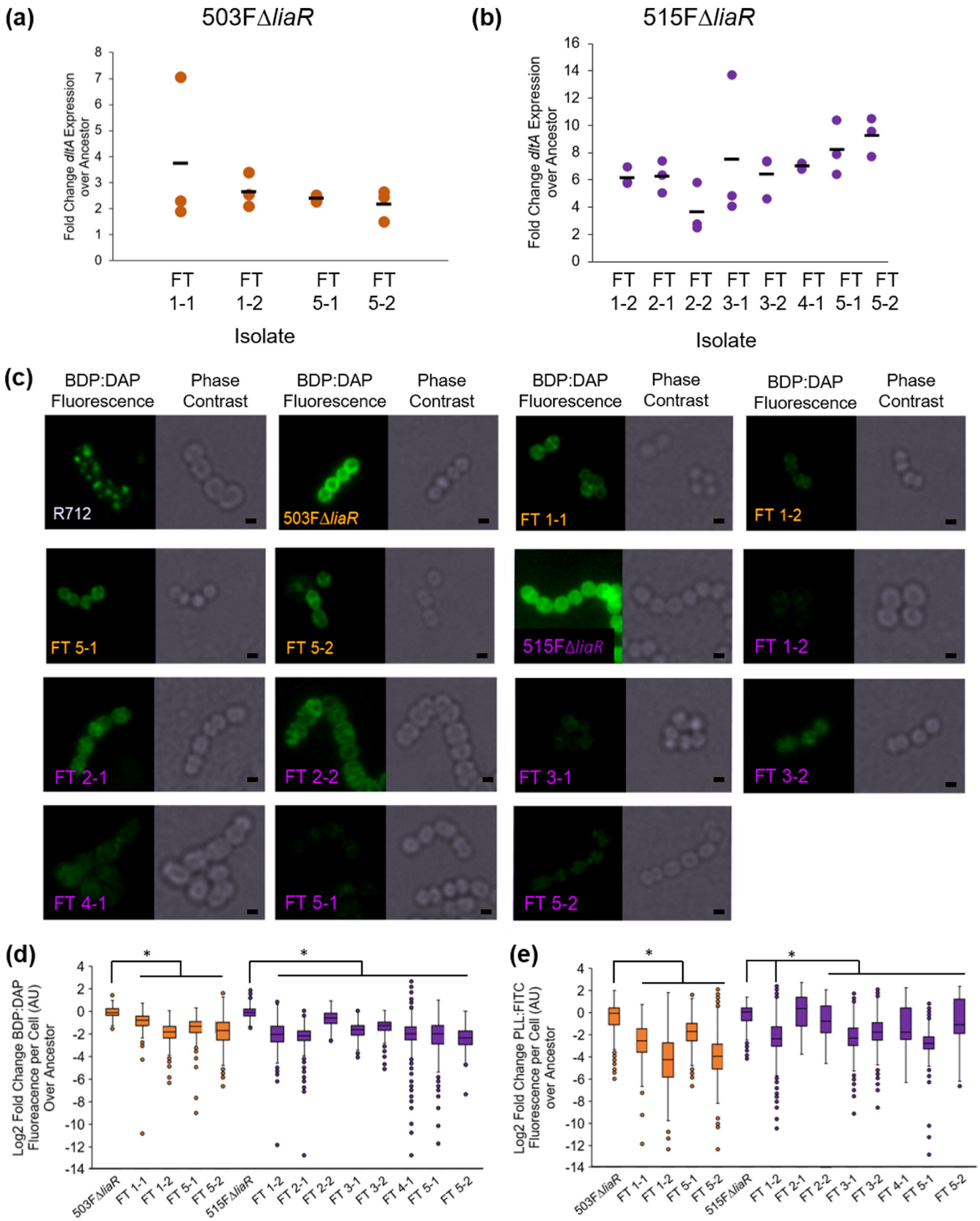

FIG 3 Flask-transfer isolates with mutations in *yvcRS* repelled DAP. (a) qPCR of *dltA* transcripts for 503FΔliaR isolates using *gdhIV* as reference. All changes were statistically significant ($P < 0.05$, Mann-Whitney *U* test). (b) qPCR of *dltA* transcripts for 515FΔliaR isolates using *gdhIV* as reference. Circles, biological

(Continued on next page)

bated with 500 nM 10-*N*-nonyl acridine orange (NAO) at 37°C with shaking in the dark for 3 h followed by three washes with 0.9% saline (9, 10, 13, 26). For all microscopy experiments, cells were resuspended in VectaShield, immobilized onto poly-L-lysine-coated coverslips, imaged on a Keyence BZ-Z710, performed in duplicate on separate days, and quantified using ImageJ.

As observed in HOU503, isolates lacking *liaR* and containing *yvcRS* mutations showed evidence of an electrostatic repulsion mechanism to confer DAP resistance (Fig. 3). Of note, without allelic replacements, the most parsimonious arguments between genotype and phenotype are shown here, where multiple isolates carrying similar mutations were assessed. In many cases, an additional variant was present within cardiolipin synthase (*cls*), which has also been identified in many evolutionary trajectories associated with DAP resistance in both redistribution and repulsion-based contexts (5, 13, 27). In Δ*liaR* flask-transfer isolates containing *yvcRS* mutations, *dltA* transcripts were significantly elevated compared with the housekeeping gene *gdhIV* and bound significantly less BDP:DAP than the ancestor without the DAP-redistribution phenotype that is associated with DAP resistance in *E. faecalis* R712 (Fig. 3a to c). To determine whether this reduction in BDP:DAP binding may be the result of increases in cell surface charge, isolates were incubated with PLL:FITC as described above. All flask-transfer (FT) isolates containing *yvcRS* mutations bound less PLL:FITC than the ancestors (except 515FΔ*liaR* FT1-2), suggesting an increase in cell surface charge (Fig. 3e; see also Fig. S1 in the supplemental material). Incubation with NAO revealed no evidence of lipid redistribution (see Fig. S2 in the supplemental material) (9, 10, 26).

Although this sampling does not provide a quantitative survey of all mutations derived from flask adaptation, the evolution of *yvcRS* mutations across different populations and ancestral genomes suggests their importance in contributing to DAP resistance independent of a functional LiaFSR system. Previously, a *yvcR* mutation was also identified in a DAP-resistant flask-transfer isolate of *E. faecalis* lacking *liaR* (12). Importantly, 503FΔ*liaR* FT1-1 ($yvcS^{A647P}$, cls^{A20D}) possessed similar mutations to HOU503 FT5 ($yvcS^{S23I}$, cls^{R218Q}) (13), yet the timeline to resistance differed markedly. So, *yvcRS* mutations allowed HOU503 to readily achieve high levels of DAP resistance (13); however, when *liaR* was deleted, the same level of resistance was not observed for an additional 2 weeks.

In a bioreactor environment with complex biofilms, both 503FΔ*liaR* and 515FΔ*liaR* evolved resistance through a multitude of mutations that resulted in various resistant phenotypes (Tables 3 and 4, Fig. 2; see also Fig. S3 to S8 in the supplemental material). Interestingly, the adaptive mutations differed between 503FΔ*liaR* and 515FΔ*liaR*. In 503FΔ*liaR* bioreactor-evolved isolates, we observed mutations affecting a wide range of mechanistic systems, including cell division (*divIVA*) (Fig. S3), cell wall synthesis (*murAA*) (Fig. S4 and S5), and lipid metabolism (*cls*). In several instances, VAN sensitivity was restored (see Text S1 and Table S1 in the supplemental material). Conversely, 515FΔ*liaR* almost exclusively evolved one of two mutations in cystathionine gamma-synthase (*metB*), both of which resulted in an extension of the open reading frame into the downstream gene cystathionine beta-lyase (*metC*). Each lineage resulted in differing phenotypes (Text S1, Fig. S6 to S8). Interestingly, both 503FΔ*liaR* and 515FΔ*liaR* evolved mutations downstream of a plasmid-encoded *repA*. Mutations downstream of *repA* were not observed in a 515FΔ*liaR* no-drug control, and the significance of these changes remains under investigation (Text S1). Importantly, although multiple trajectories

FIG 3 Legend (Continued)

replicates; bars, means. (c) Isolates were incubated with 32 μg/ml BDP-DAP. Scale bars, 1 μm. *E. faecalis* R712 acts as a control showing the DAP redistribution phenotype. (d) Quantification of BDP:DAP. (e) Quantification of PLL:FITC; images found in Fig. S1 in the supplemental material. Isolate names in orange are 503FΔ*liaR* isolates, and names in purple are 515FΔ*liaR* isolates. *, Significance compared to the ancestor ($P < 0.05$) using Mann-Whitney *U* test with *post hoc* Holm-Bonferroni adjustment. Experiment performed in duplicate on separate days. Quantification using ImageJ.

and phenotypes existed in the biofilm-heavy environment, the timeline to resistance was still significantly delayed when *liaR* was not present.

In summary, deleting *liaR* from the *E. faecium* genome greatly delayed the onset of DAP resistance. The evolved resistance mechanisms varied greatly depending on environment and ancestral genome, suggesting that activation of LiaFSR is the dominant pathway to resistance in *E. faecium*. This delay in the emergence of resistance supports the development of a LiaFSR inhibitor to be used with DAP and potentially other cell membrane active compounds.

Statistical significance was defined as $P < 0.05$ using the Mann-Whitney test with *post hoc* Holm-Bonferroni adjustment unless otherwise stated.

Data availability. All sequences are deposited under BioProject no. PRJNA549910, PRJNA551139, and PRJNA551146.

SUPPLEMENTAL MATERIAL

Supplemental material is available online only.

SUPPLEMENTAL FILE 1, PDF file, 1.3 MB.

ACKNOWLEDGMENTS

This work was supported by National Institutes of Health, National Institute of Allergy and Infectious Diseases grants R01AI080714 to Y.S., K08 AI135093 to W.R. M., K24-AI121296 and R01-AI134637 to C.A.A., and K08-AI113317 to T.T.

Funding agencies did not play a role in experimental design, performance, or analysis.

C.A.A. has received grants from Merck, MeMEd Diagnostics, and Entasis Therapeutics. W.R.M. has received grants from Merck and Entasis Therapeutics and honoraria from Shionogi.

REFERENCES

1. Robbel L, Marahiel MA. 2010. Daptomycin, a bacterial lipopeptide synthesized by a nonribosomal machinery. J Biol Chem 285:27501–27508. https://doi.org/10.1074/jbc.R110.128181.
2. Shoemaker DM, Simou J, Roland WE. 2006. A review of daptomycin for injection (Cubicin) in the treatment of complicated skin and skin structure infections. Ther Clin Risk Manag 2:169–174. https://doi.org/10.2147/tcrm.2006.2.2.169.
3. Steenbergen JN, Alder J, Thorne GM, Tally FP. 2005. Daptomycin: a lipopeptide antibiotic for the treatment of serious Gram-positive infections. J Antimicrob Chemother 55:283–288. https://doi.org/10.1093/jac/dkh546.
4. Arias CA, Panesso D, McGrath DM, Qin X, Mojica MF, Miller C, Diaz L, Tran TT, Rincon S, Barbu EM, Reyes J, Roh JH, Lobos E, Sodergren E, Pasqualini R, Arap W, Quinn JP, Shamoo Y, Murray BE, Weinstock GM. 2011. Genetic basis for in vivo daptomycin resistance in enterococci. N Engl J Med 365:892–900. https://doi.org/10.1056/NEJMoa1011138.
5. Miller C, Kong J, Tran TT, Arias CA, Saxer G, Shamoo Y. 2013. Adaptation of *Enterococcus faecalis* to daptomycin reveals an ordered progression to resistance. Antimicrob Agents Chemother 57:5373–5383. https://doi.org/10.1128/AAC.01473-13.
6. Panesso D, Reyes J, Gaston E, Deal M, Londoño A, Nigo M, Munita JM, Miller W, Shamoo Y, Tran TT, Arias CA. 2015. Deletion of *liaR* reverses daptomycin resistance in *Enterococcus faecium* independent of the genetic background. Antimicrob Agents Chemother 59:7327–7334. https://doi.org/10.1128/AAC.01073-15.
7. Diaz L, Tran TT, Munita JM, Miller WR, Rincon S, Carvajal LP, Wollam A, Reyes J, Panesso D, Rojas NL, Shamoo Y, Murray BE, Weinstock GM, Arias CA. 2014. Whole-genome analyses of *Enterococcus faecium* isolates with diverse daptomycin MICs. Antimicrob Agents Chemother 58:4527–4534. https://doi.org/10.1128/AAC.02686-14.
8. Tran TT, Panesso D, Gao H, Roh JH, Munita JM, Reyes J, Diaz L, Lobos E. a, Shamoo Y, Mishra NN, Bayer AS, Murray BE, Weinstock GM, Arias CA. 2013. Whole-genome analysis of a daptomycin-susceptible *Enterococcus faecium* strain and its daptomycin-resistant variant arising during therapy. Antimicrob Agents Chemother 57:261–268. https://doi.org/10.1128/AAC.01454-12.
9. Reyes J, Panesso D, Tran TT, Mishra NN, Cruz MR, Munita JM, Singh KV, Yeaman MR, Murray BE, Shamoo Y, Garsin D, Bayer AS, Arias CA. 2015. A liaR deletion restores susceptibility to daptomycin and antimicrobial peptides in multidrug-resistant Enterococcus faecalis. J Infect Dis 211:1317–1325. https://doi.org/10.1093/infdis/jiu602.
10. Tran TT, Panesso D, Mishra NN, Mileykovskaya E, Guan Z, Munita JM, Reyes J, Diaz L, Weinstock GM, Murray BE, Shamoo Y, Dowhan W, Bayer AS, Arias CA. 2013. Daptomycin-resistant *Enterococcus faecalis* diverts the antibiotic molecule from the division septum and remodels cell membrane. mBio 4:1–10. https://doi.org/10.1128/mBio.00281-13.
11. Tran TT, Miller WR, Shamoo Y, Arias CA. 2016. Targeting cell membrane adaptation as a novel antimicrobial strategy. Curr Opin Microbiol 33:91–96. https://doi.org/10.1016/j.mib.2016.07.002.
12. Miller WR, Tran TT, Diaz L, Rios R, Khan A, Reyes J, Prater AG, Panesso D, Shamoo Y, Arias CA. 2019. LiaR-independent pathways to daptomycin resistance in Enterococcus faecalis reveal a multilayer defense against cell envelope antibiotics. Mol Microbiol 111:811–824. https://doi.org/10.1111/mmi.14193.
13. Prater AG, Mehta HH, Kosgei AJ, Miller WR, Tran TT, Cesar A, Shamoo Y. 2019. Environment shapes the accessible daptomycin resistance mechanisms in *Enterococcus faecium*. Antimicrob Agents Chemother 63:e00790-19. https://doi.org/10.1128/AAC.00790-19.
14. Mehta HH, Prater AG, Shamoo Y. 2018. Using experimental evolution to identify druggable targets that could inhibit the evolution of antimicrobial resistance. J Antibiot 71:279–286. https://doi.org/10.1038/ja.2017.108.
15. Hammerstrom TG, Beabout K, Clements TP, Saxer G, Shamoo Y. 2015. Acinetobacter baumannii repeatedly evolves a hypermutator phenotype in response to tigecycline that effectively surveys evolutionary

trajectories to resistance. PLoS One 10:e0140489. https://doi.org/10.1371/journal.pone.0140489.
16. Beabout K, Hammerstrom TG, Wang TT, Bhatt M, Christie PJ, Saxer G, Shamoo Y. 2015. Rampant parasexuality evolves in a hospital pathogen during antibiotic selection. Mol Biol Evol 32:2585–2597. https://doi.org/10.1093/molbev/msv133.
17. Mehta HH, Weng J, Prater AG, Elworth RAL, Han X, Shamoo Y. 2018. Pathogenic *Nocardia cyriacigeorgica* and *Nocardia nova* evolve to resist trimethoprim-sulfamethoxazole by both expected and unexpected pathways. Antimicrob Agents Chemother 62:e00364-18. https://doi.org/10.1128/AAC.00364-18.
18. Mehta HH, Prater AG, Beabout K, Elworth RAL, Karavis M, Gibbons HS, Shamoo Y. 2019. The essential role of hypermutation in rapid adaptation to antibiotic stress. Antimicrob Agents Chemother 63:e00744-19. https://doi.org/10.1128/AAC.00744-19.
19. Beabout K, Hammerstrom TG, Perez AM, Magalhães BF, Prater AG, Clements TP, Arias CA, Saxer G, Shamoo Y. 2015. The ribosomal S10 protein is a general target for decreased tigecycline susceptibility. Antimicrob Agents Chemother 59:5561–5566. https://doi.org/10.1128/AAC.00547-15.
20. Barrick JE, Lenski RE. 2013. Genome dynamics during experimental evolution. Nat Rev Genet 14:827–839. https://doi.org/10.1038/nrg3564.
21. Pogliano J, Pogliano N, Silverman JA. 2012. Daptomycin-mediated reorganization of membrane architecture causes mislocalization of essential cell division proteins. J Bacteriol 194:4494–4504. https://doi.org/10.1128/JB.00011-12.
22. Hachmann A-B, Angert ER, Helmann JD. 2009. Genetic analysis of factors affecting susceptibility of *Bacillus subtilis* to daptomycin. Antimicrob Agents Chemother 53:1598–1609. https://doi.org/10.1128/AAC.01329-08.
23. Hachmann AB, Sevim E, Gaballa A, Popham DL, Antelmann H, Helmann JD. 2011. Reduction in membrane phosphatidylglycerol content leads to daptomycin resistance in *Bacillus subtilis*. Antimicrob Agents Chemother 55:4326–4337. https://doi.org/10.1128/AAC.01819-10.
24. Pader V, Hakim S, Painter KL, Wigneshweraraj S, Clarke TB, Edwards AM. 2016. Staphylococcus aureus inactivates daptomycin by releasing membrane phospholipids. Nat Microbiol 2:16194. https://doi.org/10.1038/nmicrobiol.2016.194.
25. Hartmann W, Galla H-J. 1978. Binding pf polylysine to charged bilayer membranes molecular organization of a lipid:peptide complex. North Holl Biomed Press 509:474–490. https://doi.org/10.1016/0005-2736(78)90241-9.
26. Barák I, Muchová K. 2013. The role of lipid domains in bacterial cell processes. Int J Mol Sci 14:4050–4065. https://doi.org/10.3390/ijms14024050.
27. Davlieva M, Zhang W, Arias CA, Shamoo Y. 2013. Biochemical characterization of cardiolipin synthase mutations associated with daptomycin resistance in enterococci. Antimicrob Agents Chemother 57:289–296. https://doi.org/10.1128/AAC.01743-12.